Orthorhombic lattice deformation of $GdSr_2RuCu_2O_8$ from high-resolution transmission electron microscopy and x-ray powder diffraction analysis

A. Martinelli,[1,*] C. Artini,[2] M. R. Cimberle,[3] G. A. Costa,[2] M. Ferretti,[2] R. Masini,[3] and P. Mele[2]
[1]*LAMIA, National Institute for the Physics of Matter (INFM), C.so Perrone 24, I-16152, Genova, Italy*
[2]*LAMIA–INFM and Dipartimento di Chimica e Chimica Industriale, Via Dodecaneso 31, I-16146, Genova, Italy*
[3]*CNR-IMEM sezione di Genova c/o Dipartimento di Fisica, Via Dodecaneso 33, I-16146, Genova, Italy*
(Received 21 February 2003; revised manuscript received 20 May 2003; published 27 February 2004)

$GdSr_2RuCu_2O_8$ has been synthesized using a solid state reaction and has been characterized from the structural and physical points of view. The samples exhibit the well-known superconducting and magnetic behavior; in addition, an orthorhombic modification of the $GdSr_2RuCu_2O_8$ lattice has been detected by both high resolution transmission electron microscopy (HRTEM) and x-ray powder diffraction (XRPD) analysis. Rietveld refinement of the XRPD data has been successfully performed in the orthorhombic *Pmmm* space group yielding an $a_0 \times b_0 \times c_0 (\approx 3\, a_0)$ type cell, with octahedral RuO_6 polyhedra slightly distorted and rotated around *c*, *b*, and *a*.

DOI: 10.1103/PhysRevB.69.052507 PACS number(s): 74.70.Pq, 74.72.−h, 68.37.Lp, 61.10.Nz

I. INTRODUCTION

Ruthenocuprates of the $RuSr_2LCu_2O_8$ type (Ru-1212; L = Sm, Eu, Gd) constitute an attractive class of compounds exhibiting the coesistence of both superconductivity and magnetism, two types of long-range ordering which have always been considered to be antagonist. For this reason, since its first synthesis,[1] intensive experimental work has been devoted to this phase (in particular with L = Gd or, to a lesser extent, Eu) to elucidate various problems: the structural and microstructural homogeneity (i.e., the existence of a unique phase exhibiting the coexistence of magnetic and superconducting ordering), the type of magnetic ordering (for which contrasting indications are obtained through different experimental techniques), and the valence state of ruthenium. All these issues are still being discussed.

In addition, it is well known that the physical properties are strongly ''sample dependent'' in spite of the structural invariance of the samples, at least as far as can be observed with the standard crystallographic characterization techniques.[2] It has been argued that the observed differences in the physical behaviors must depend on subtle structural details. Therefore, an accurate structural study of this phase is imperative.

The structure of the Ru-1212-type compounds may be regarded as being derived from that of $YBa_2Cu_3O_{7-\delta}$, with Ru replacing the Cu atoms located in the charge reservoir layer in their crystallographic sites; structural investigations are based on the refinement of powder diffraction data, with the assumption of a tetragonal *P*4/*mmm* (space group: 123) (Refs. 3–6) or *P*4/*mbm* (space group: 127) structure.[4]

In this work high resolution transmission electron microscopy and x-ray powder diffraction data are reported and discussed. They highlight an orthorhombic lattice modification of $GdSr_2RuCu_2O_8$ samples, showing the expected superconductive and magnetic properties.

II. EXPERIMENTAL

The $GdSr_2RuCu_2O_8$ phase was prepared by the method reported in Ref. 7, i.e., by a standard solid state reaction procedure that involves a long series of subsequent grindings and annealings at increasing temperature, aimed to avoid the formation of spurious phases and to increase the homogeneity of the sample. The sample thus prepared was divided into different parts that underwent different annealing treatments: one part was annealed in fluent oxygen at $T = 1335$ K for 1 week, and another one for 1 month in the same conditions. Inelastic spectroscopy measurements[8] revealed that the samples had been prepared with very low O deficiency (referring to an ideal formula $GdSr_2RuCu_2O_{8-\delta}$, $\delta < 0.2\%$).

Structural and microstructural characterizations were performed by means of HRTEM Jeol JEM-2010 operated at 200 kV and equipped with an Oxford Pentafet energy-dispersive x-ray spectrometer system and by means of XRPD Philips PW1830 in Bragg-Brentano geometry (CuK_α radiation, secondary monochromator, 2θ range: 13–80°; step: 0.020° 2θ; sampling time: 15 sec). The samples were characterized by resistivity and magnetic measurements using a standard four-probe technique and a Quantum Design SQUID magnetometer, respectively. They exhibit a magnetic transition at about 130 K and a superconducting transition with an onset at about 45 K.

The crystal structure was refined in the *Pmmm* (No. 47) space group according to the Rietveld method[9] using the DBWS9006 program. The stoichiometry was set to the ideal $GdSr_2RuCu_2O_8$ composition. In order to minimize size contribution to diffraction lines broadening and hence their overlapping, the XRPD pattern of $GdSr_2RuCu_2O_8$ sample reannealed for 1 month was used for profile fitting of diffraction lines in the 22.7–23.7° 2θ range, using pseudo-Voigt functions (step: 0.005° 2θ; sampling time: 45 sec).

III. RESULTS AND DISCUSSION

A. Resistive and magnetic characterization

Figure 1 shows the resistive (*a*) and magnetic (*b*) characterization of the sample annealed for 1 week, chosen as representative and exhibiting the typical properties of the Ru-(1212) phase.[4] As temperature decreases, resistivity

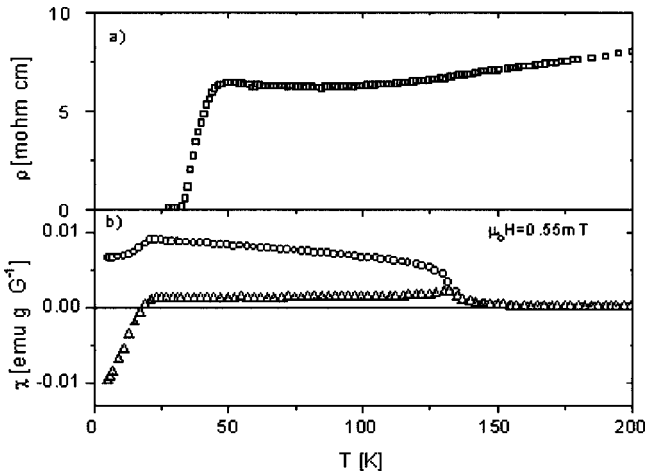

FIG. 1. (a) Zero field resistivity and (b) ZFC (triangles) and FC (circles) magnetic susceptibility versus temperature at $\mu_0 H = 0.55$ mT.

shows a metallic behavior and a slight semiconducting upturn before the superconducting transition, which has the onset at about $T = 45$ K and a width of about 13 K [$T(\rho = 0) = 32$ K]. The magnetic susceptibility indicates a magnetic ordering at about $T = 130$ K and a superconducting transition. The onset of the superconducting transition is observed at about $T = 40$ K from the derivative of susceptibility with respect to temperature; an evident diamagnetic behavior, both in zero field cooled and field cooled conditions, is seen below $T < 25$ K where the grains become connected through weak links. At the applied field $\mu_0 H = 0.55$ mT, the diamagnetic shielding corresponds to a value $\chi = -0.45$ while the Meissner effect corresponds to $\chi = -0.095$.

B. TEM observation

In general, the orthorhombic structure may be detected on HRTEM images and selected area electron diffraction (SAED) patterns collected along the [001] zone axis; the small difference between a_0 and b_0 may be revealed by the direct measurement of the periodicities of the lattice fringes. Figure 2 shows a HRTEM image of a $GdSr_2RuCu_2O_8$ particle, in which three different domains (A, B, and C) characterized by different lattice orientation may be distinguished: in particular, A and C are viewed along [010], rotated by 90° with respect to each other. In the third domain B the structure is viewed under [001]; the periodicity of the lattice fringes in this domain reveals that the ratio $b_0/a_0 \sim 0.98$. Furthermore, at the boundary between the B and C domains the strain-free transformation of a (001) fringe into three (100) fringes may be observed; on the contrary, at the boundary between the A and C domains lattice strain occurs, because of the mismatch between the $3b_0$ and c_0 values. Figure 3 shows the same region of Fig. 2 collected with a different defocus value, exhibiting coherent (103) lattice fringes running from A to C throughout B; at higher magnification, these fringes show a little distortion at the boundary separating A from C.

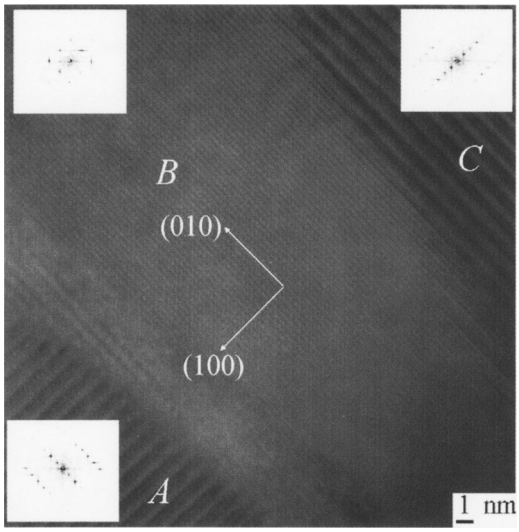

FIG. 2. HRTEM images of a $GdSr_2RuCu_2O_8$ particle showing three different domains (A, B, and C); the insets show the fast Fourier transforms of the corresponding domains.

C. XRPD analysis and Rietveld refinement

The diffraction pattern is similar to those reported in the literature for the tetragonal structure and reveals a high purity degree of the product, since only the presence of $GdSr_2RuCu_2O_8$ may be detected; the amount of other phases, if present, are below the instrumental limit of detection. In the light of the TEM analysis results, evidence for orthorhombic structure has been searched for in the XRPD pattern. An accurate investigation of the diffraction pattern in the 22.7–23.7° 2θ region reveals the presence of a strongly asymmetric peak; the asymmetry cannot be attributed to $K_{\alpha 1}$ and $K_{\alpha 2}$ splitting, since the broadening is towards the low

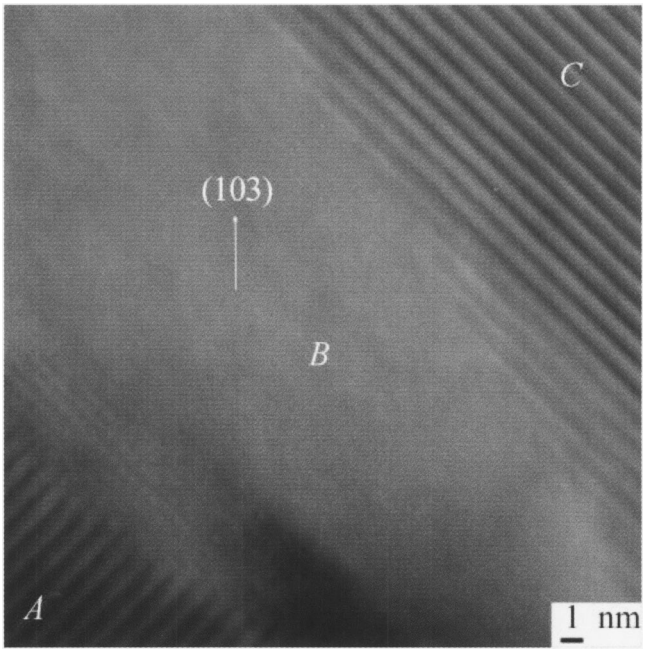

FIG. 3. The same region of the Fig. 2 at a different defocus value.

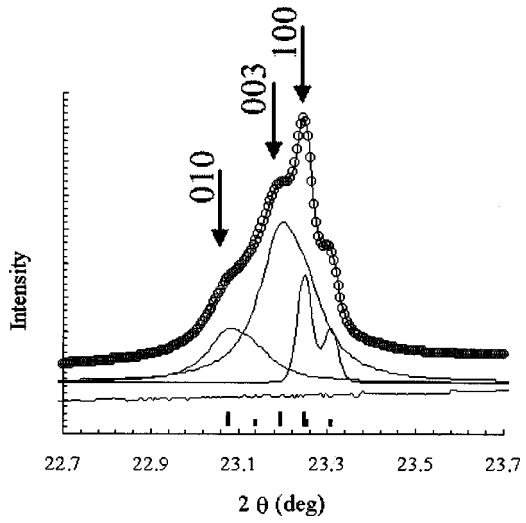

FIG. 4. Indexed and fitted XRPD patterns collected in the 22.7–23.7° 2θ region: three overlapping reflections come out. Observed and calculated profile intensities are represented by ∅ and solid lines, respectively, their difference is plotted below as a solid line; vertical bars represent the positions of the Bragg reflections for $K_{\alpha 1}$ and $K_{\alpha 2}$.

angles, but is related to the superposition of different reflections. The pattern decomposition reveals the existence of three partially superposed peaks (Fig. 4), whereas, if the structure were tetragonal, only two lines should be detected (100 and 003). Pattern decomposition in this range turns out to be difficult because of the weakness of reflections, the consequent relatively high statistical noise and their close overlapping; as a consequence the accuracy of the profile fit is strongly reduced, even though three distinct diffracting planes may be distinguished, corresponding to 010, 003, 100.

Figure 5 shows the Rietveld plot after refinement in the *Pmmm* (No. 47) space group; the cell size data and R_{wp} values are summarized in Table I. Rietveld refinement confirms an $a_0 \times b_0 \times c_0 (\approx 3\, a_0)$ type cell, although the value of

TABLE I. Cell size data, positional parameters, and R_{wp} from Rietveld refinement for $GdSr_2RuCu_2O_8$.

a (Å)	b (Å)	c (Å)	V (Å^3)	R_{wp}
3.8293(2)	3.8488(2)	11.5026(7)	169.528	0.0554

the ratio $b_0/a_0 (\sim 0.995)$ has increased with respect to the HRTEM result. The cationic sublattice of orthorhombic $GdSr_2RuCu_2O_8$ may be regarded as directly derived from that of orthorhombic $YBa_2Cu_3O_{7-x}$, with Gd and Sr replacing Y and Ba in their crystallographic sites, respectively, and Ru occupying one of the two sites of Cu. As a result, an octahedral sheet is obtained, where slightly distorted octahedral polyhedra with rectangular planes are coordinated by Ru and rotated around c by $\sim 15.2°$ and around b and a by $\sim 4.7°$. In the light of this, the ordering of the structural vacancies in the O sublattice may lead to the formation of superstructures, as revealed by electron diffraction patterns obtained during our investigation (details will be given elsewhere). It is worth remarking that the distinction between a tetragonal and orthorhombic structure is very subtle and is better revealed by accurate analysis of HRTEM images and SAED patterns obtained along [001]; on the other hand, the XRPD could be successfully indexed according to a tetragonal cell. The Rietveld refinement can be performed in the *P4/mmm* space group and in this case the lattice parameters are $a = 3.8354(2)$ and $c = 11.5684(7)$.

It is not clear whether the orthorhombic structure of $GdSr_2RuCu_2O_8$ has ever been reported in the previous works because of its extremely problematic detection, enhanced by the lack of single-crystal XRD data, or if the orthorhombic and the tetragonal structures may both exist. At present only careful HRTEM observation along the [001] direction can help ascertain the crystal system to which $GdSr_2RuCu_2O_8$ belongs. Thus, further investigations are needed for the exact structural resolution of this phase.

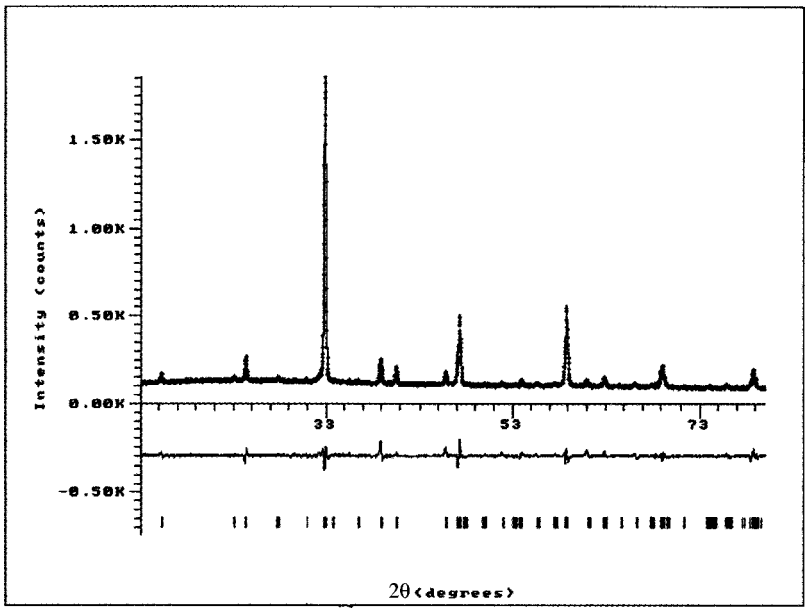

FIG. 5. Rietveld refinement plot for $GdSr_2RuCu_2O_8$: the observed intensity data and the calculated pattern are plotted in the upper field as points and solid-line curve, respectively; their difference is in the middle field, the positions of the possible Bragg reflections are in the lower field.

IV. CONCLUSIONS

$GdSr_2RuCu_2O_8$ was prepared by means of a solid state reaction with a high degree of purity: HRTEM observations performed on different samples do not evidence the presence of secondary or intergrowth phases. The samples exhibit both superconductive and magnetic properties. The orthorhombic structure of $GdSr_2RuCu_2O_8$ has been revealed by a coupling TEM analysis with the Rietveld refinement method and pattern decomposition from XRPD data; the structure may be regarded as derived from that of orthorhombic $YBa_2Cu_3O_{7-x}$ with some important differences in the O sublattice; from HRTEM images and Rietveld refinement an $a_0 \times b_0 \times c_0 (\approx 3\, a_0)$ cell is apparent, crystallizing in the $Pmmm$ space group. On the other hand, the Rietveld refinement may be successfully performed in the tetragonal $P4/mmm$ space group; as a result of this, the value of the parameter a for the tetragonal structure is between the values of a and b for the orthorhombic structure, whereas the value of the parameter c for the tetragonal structure slightly exceeds that of the orthorhombic structure. We would like to point out that small structural differences may be of importance when trying to understand the physics of this system that involves a complex and as of yet unclarified magnetic ordering and coexistence of magnetic and superconducting ordering.

*Email address: amartin@chimica.unige.it

[1] L. Bauernfeind, W. Widder, and H.F. Braun, Physica C **254**, 151 (1995).
[2] P.W. Klamuth *et al.*, *Lecture Notes in Physics* (Springer-Verlag, Berlin, 2002).
[3] A.C. McLaughlin, W. Zhou, J.P. Attfield, A.N. Fitch, and J.L. Tallon, Phys. Rev. B **60**, 7512 (1999).
[4] O. Chmaissem, J.D. Jorgensen, H. Shaked, P. Dollar, and J. L. Tallon, Phys. Rev. B **61**, 6401 (2000).
[5] G.M. Kuz'micheva, V.V. Luparev, E.P. Khlybov, I.E. Kostyleva, A.S. Andreenko, and K.N. Gavrilov, Physica C **350**, 105 (2001).
[6] V.P.S. Awana, S. Ichihara, J. Nakamura, M. Karppinen, H. Yamauchi, Jinbo Yang, W.B. Yelon, W.J. James, and S.K. Malik, J. Appl. Phys. **91**, 8501 (2002).
[7] C. Artini, M.M. Carnasciali, G.A. Costa, M. Ferretti, M.R. Cimberle, M. Putti, and R. Masini, Physica C **377**, 431 (2002).
[8] F. Cordero, M. Ferretti, M.R. Cimberle, and R. Masini, Phys. Rev. B **67**, 144519 (2003).
[9] R.A. Young, in *The Rietveld Method* edited by R.A. Young, Vol. 5 of *IUCr Monographs on Crystallography* (Oxford University Press, Oxford, 1993), Chap. 1, pp. 1–38.